HOKKAIDO UNIVERSITY

Title	Electrochemical Formation of Self-Assembled InP Nanopore Arrays and Their Use as Templates for Molecular Beam Epitaxy Growth of InGaAs Quantum Wires and Dots
Author(s)	Hirano, Tetsuro; Ito, Akira; Sato, Taketomo et al.
Citation	Japanese Journal of Applied Physics part 1, Regular papers & short notes, 41(2B), 977-981 https://doi.org/10.1143/JJAP.41.977
Issue Date	2002-02
Doc URL	https://hdl.handle.net/2115/33093
Rights	Copyright © 2002 The Japan Society of Applied Physics
Type	journal article
File Information	JJAP1~41-2B.pdf

Hokkaido University Collection of Scholarly and Academic Papers : HUSCAP

Japanese Journal of Applied Physics, 41-2B (2002) 977

Electrochemical Formation of Self-Assembled InP Nanopore Arrays and Their Use as Templates for Molecular Beam Epitaxy Growth of InGaAs Quantum Wires and Dots

Tetsuro Hirano[1*], Akira Ito [1], Taketomo Sato [2], Fumitaro Ishikawa [1] and Hideki Hasegawa[1,2]

[1]*Graduate School of Electronics and Information Engineering Hokkaido University, North-13, West-8, Sapporo 060-8628, Japan*
[2]*Research Center for Integrated Quantum Electronics, Hokkaido University, North-13, West-8, Sapporo 060-8628, Japan*
*Corresponding author. E-mail address: hirano@rciqe.hokudai.ac.jp

Abstract

Attempts were made to optimize the parameters of the electrochemical process to form uniform nanopore arrays and utilize them as templates for molecular beam epitaxy (MBE) growth of InP-based quantum wires and quantum dots. Template parameters such as pore depth, diameter and period were strongly dependent on anodization conditions. In particular, in the pulsed anodization mode, the pore depth could be well controlled in the nanometer range by adjusting the number of the applied pulses. InGaAs MBE growth was attempted using the nanopore templates. Growth of InGaAs in pores occurred at a substantial depth of about 20-60 nm. The measured photoluminescence (PL) spectra had a new peak at about 1.2 eV in addition to the PL emission from the InP substrate and that from the InGaAs top layer. The new peak was tentatively assigned to the peak arising from InGaAs quantum wire arrays embedded in InP pores with a possible alloy composition change.

KEYWORDS: nanopore, template, porous InP, InGaAs, MBE growth, PL, electrochemical anodization

1. Introduction

Recently, semiconductor quantum wire (QWR) and quantum dot (QD) structures have been attracting attention for applications to new electronic and optoelectronic devices based on quantum mechanics. For the fabrication process of QWRs and QDs, the size and position controllability, and the density as well as absence of processing damage are the key factors. The standard approach for forming arrays of semiconductor QWRs and QDs is either self-assembled crystal growth, or selective crystal growth on suitable templates. The former enables high-density formation but not position and size controllability, while the latter enables position and size controllability but not that of density due to low-density templates produced by lithography.

A possible new approach is to use self-assembled high-density nanopore arrays produced by electrochemical anodization as templates for crystal growth. Previously, it has been reported that anodization of Al can produce in a self-assembled fashion, anodic porous alumina containing a well-ordered array of air holes with a period of 100 nm or below[1,2]. However, as for silicon and III-V semiconductors[3,4], it is known that anodized porous structures have random fractal-like structures typically seen in anodized porous Si, and the method for obtaining regular periodic arrays of nanopore structural controllability has not been found yet except our recent reports[5,6].

The purpose of this paper is to explore the possibilities of forming high-density, regular and straight nanopore arrays on InP by electrochemical anodization, and to try to use them as templates for molecular beam epitaxy (MBE) growth of high-density QWRs and QDs. Their structures are shown in **Fig. 1**. Structural uniformity and controllability of nanopore templates and MBE grown structures were investigated in detail by scanning electron microscopy (SEM). Their optical properties were investigated by the photoluminescence (PL) method.

2. Experimental

The setup of the electrochemical anodization process used for the fabrication of nanopore arrays was shown in **Fig. 2(a)**. The electrochemical cell had three electrodes, namely, an n-InP electrode (n =1.5x10^{18} cm^{-3}), a Pt counter electrode and a reference saturated calomel electrode (S.C.E). The overpotential, V_s, on the InP electrode was controlled with respect to the S.C.E. by a potenstiostat. Three types of electrolytes, A: 1M HCl (200 ml), B: 1M HCl (200 ml) + H_2PtCl_6 (1 g) and C: 1M HCl (200 ml) + HNO_3 (3 ml), were used. For the current supply to the InP electrode, a GeAu/Ni ohmic contact was made on the back surface of the n-InP substrate by a conventional metal evaporation and annealing process at 370˚C for 5 min. Immediately before anodization, sulfuric acid-based wet etching was carried out. Using a standard solution of H_2SO_4 : H_2O_2 : H_2O = 3 : 1 : 1 yielded an n-InP substrate with a rms surface roughness value of approximately less than 10 nm as determined by atomic force microscopy (AFM) measurement. In this study, d.c. bias mode and pulsed bias mode shown in **Fig. 2(b)** were used for the formation of nanopore arrays. In the d.c. mode, the overpotential V_s and the anodization time t_a were changed within ranges of 4-9 V and 0.1-180 s, respectively. In the pulsed mode, the overpotential V_s, pulse width t_w and pulse period t_p were set at 7 V, 0.1 s and 1.0 s, respectively, and the anodization time was controlled by adjusting the number of pulses.

After optimization of the fabrication process of the nanopore templates, InGaAs growth was carried out using a conventional solid-source MBE system. The supply rate for each group III source was controlled in order to grow an $In_{0.53}Ga_{0.47}As$ layer lattice-matched to InP on a planar reference substrate at a growth rate of 10 nm/min. Immediately before introducing a sample into the MBE chamber, native oxides on the sample surface were removed using an HF solution for 1 min. During the MBE growth, the substrate was rotated in order to suppress non-uniformities.

SEM and PL measurements were used to characterize structural and optical properties of all the samples fabricated in this study. PL measurements were carried out using a 514.5 nm line of an Ar^+ laser as the excitation source. The diameter of the laser spot on the sample surface was 0.2 mm and the power was 30 mW.

3. Results and Discussion

3.1 Formation of nanopore array templates

In order to see whether regular nanopore arrays that are suitable as templates for MBE growth of QWRs and QDs can be found, various nanopores were initially fabricated in the d.c. mode by changing the overpotential V_s and the anodization time t_a, and their structures were investigated in detail. When V_s was above 4 V, uniform arrays of round nanopores or square nanopores with four {100} facets were formed as shown in **Fig. 3(a)**. Under optimum conditions, waving of pore direction could be suppressed and the pores became extremely straight with surprisingly small spatial variations of pore size and periodicity, as shown in **Fig. 3(b)**. However, part of the irregular top layer shown in **Fig. 3(c)** still exhibited waving. It appeared to be essential to remove this disordered top layer for application to templates.

Furthermore, it was also found that template parameters such as pore depth, diameter and period were strongly dependent on anodization conditions. The major results in the d.c mode are summarized in **Figs. 4(a)-4(c)**. The pore depth increased with anodization time at a rate of approximately 0.5 μm/s without changing the average pore diameter and period. On the other hand, the average pore size increased from 50 to 200 nm, and the average pore period also increased from 100 to 300 nm with the increase in V_s from 4 to 9 V.

The observed behavior that the pore layer depth increased as a function of time without changing the average pore diameter can be explained by the carrier supply-limited model. Namely, when the pore wall gets sufficiently thin, carriers (holes) responsible for the electrochemical etching are completely depleted in the wall region, and electrochemical reaction

no longer occurs on the surface of the pore wall.

The observed change in anodization current with anodization time is shown in **Fig. 5** for the d.c mode. A very large current flowed at the beginning, and then, the current decreased rapidly, reaching a more or less constant value.

In order to further control the pore depth in the nanometer range by avoiding this very large initial current that causes initial rapid electrochemical reaction, the pulsed bias mode was investigated for nanopore fabrication. **Figure 6(a)** shows a cross-sectional SEM image of the nanopore array fabricated in the pulsed mode. As compared to the straight pores fabricated in the d.c. mode, many knots are clearly seen in the nanopore array formed in the pulsed mode. Furthermore, it was found that the number of knots is equal to the number of pulses applied. When only one pulse is applied to the substrate, a knot-free porous template with a shallow depth can be obtained. **Figure 6(b)** shows the correlation between the depth of nanopores and the number of pulses applied under the conditions of V_s = 7 V, t_w = 0.1 s and t_p = 1.0 s. Electrolyte C was used. As the number of pulses applied increased further, the increase in the nanopore depth by each pulse addition decreased considerably at first, and gradually became almost constant as shown in **Fig. 6(b)**. Considering the current determined, it seems that the anodization reaction proceeds rapidly at the early stage and quickly reaches steady state.

In the case of the pulsed mode, it was possible to control pore depth by adjusting the number of pulses. Based on these results, it was found that the InP nanopore structure could be controlled well by optimizing the electrochemical anodization conditions. The optimized nanopore structures seemed to be very suitable as a template for MBE growth

4.2 InGaAs MBE growth on template

For MBE growth, the templates should have shallow pore arrays to ensure that growing InGaAs species diffuse into pores. For this purpose, electrochemical anodization for shallow nanopores was performed under the conditions of V_s = 7 V, t_w= 0.2 s and t_p =1.0 s with only one pulse using electrolyte C. The cross-sectional SEM image of the template obtained under these conditions is shown in **Fig. 7(a)**. This template had an average pore depth of about 600 nm and an average pore diameter of about 100 nm. Using such templates, MBE growth of $In_{0.53}Ga_{0.47}As$ was attempted. After MBE growth on the InP template, cross-sectional etching was carried out with a phosphoric acid-based solution (H_3PO_4 : H_2O_2 : H_2O = 1 : 1 : 38) for about 5 s. The cross-sectional SEM image of the grown layer is shown in **Fig. 7(b)**. By comparison with the template before MBE growth, growth of $In_{0.53}Ga_{0.47}As$ into pores clearly occurred to a substantial depth and a diameter of about 20-60 nm between the InGaAs top layer and the InP porous template. By further adjusting the growth conditions including group III supply rates, it seems possible to make completely embedded QWRs and QDs.

4.3 PL properties of InGaAs on n-InP template

The measured PL spectrum of the InGaAs/template sample is shown in **Fig. 8**. In contrast to the nanostructures formed by dry etching, the present porous InP template showed an intense red-shifted PL emission at low temperature, as reported previously[6]. However, this red-shifted PL emission disappeared, and a new broad peak appeared after MBE growth. Namely, the PL peak at 0.78 eV in **Fig. 8** arising from the top InGaAs layer is the small emission peak at 1.40 eV arising from the InP substrate underneath. In addition to these peaks, a new PL peak, which is fairly large and broad compared to the InP peak, was observed at about 1.2 eV between the InP peak and the InGaAs peak. This emission seems to arise the quantum-confined InGaAs dot-like wire segments of 20-60 nm dimensions embedded in InP fabricated by MBE growth on the InP nanopore template. As a reference data, arrowhead- shaped InGaAs ridge QWRs formed by our group on patterned InP substrates by selective MBE show PL emission at 1.0-1.2 eV for the effective wire width values of 35-10 nm[7,8]. Thus, the emission range observed in this study is similar to those observed in QWRs. Taking account of the fact that the present structure is more similar to an array of InGaAs QDs with three dimensional confinement rather than to QWRs,

and that the dot sizes change over a wide range with some dots being very small, it is not unreasonable to assign the observed broad PL peak to the peak arising from InGaAs QDs embedded in InP nanopores. Emission is rather strong for a thin QD region as compared with a much thicker InGaAs top layer. However, there may also be some alloy composition change in the QD accompanying strain.

Intensive efforts are being made to form more regular and less defective structures by further optimizing templates and MBE growth conditions.

5. Conclusions

In this study, we attempted to optimize the parameters of the electrochemical process to form uniform nanopore arrays in order to utilize them as templates for MBE growth of InP-based QWR.

(1) It is possible to control pore depth, pore diameter and pore period by adjusting electrochemical reaction time and anodic voltage. The carrier supply-limited model can explain this behavior.

(2) In the pulsed mode, it is possible to control pore depth by adjusting the number of pulses.

(3) Growth of InGaAs in the pore occurs during MBE growth on InP porous substrate.

(4) The measured PL spectrum from the InGaAs/InP porous template sample has a new peak that seems to arise from the InGaAs wire segment embedded in the InP nanopores.

References

1) H. Masuda, K. Yada and A. Osaka: Jpn. J. Appl. Phys. **37** (1998) 1340.
2) H. Masuda, M. Ohya, H. Asoh and M. Nakao: Jpn. J. Appl. Phys. **38** (1999) 1403.
3) R. L. Smith and S. D. Collins: J. Appl. Phys. **8** (1992) R1
4) M. I. J. Beale, N. G. Chew, M. J. Uren, A. G. Cullis and J. D. Benjamin: Appl. Phys. Lett. **46** (1985) 86.
5) A. Hamamatsu, C. Kaneshiro, H. Fujikura and H. Hasegawa: J. Electroanalytic. Chem. **473** (1999) 223.
6) H. Fujikura, A. Liu, A. Hamamatsu, T. Sato and H. Hasegawa: Jpn. J. Appl. Phys. **39** (2000) 4616.
7) C. Jiang, T. Muranaka and H. Hasegawa: Jpn. J. Appl. Phys. **40** (2001) 3003
8) C. Jiang, T. Muranaka and H. Hasegawa: Proc. 13th Int. Conf. Indium Phosphide and Related Materials (2001) p. 374.

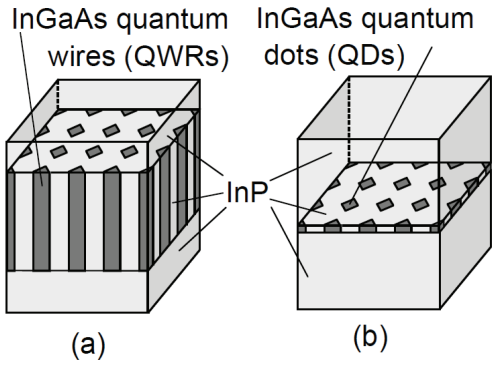

Fig. 1 High-density (a) QWR array and (b) QD array structures of electrochemically produced nanopore templates.

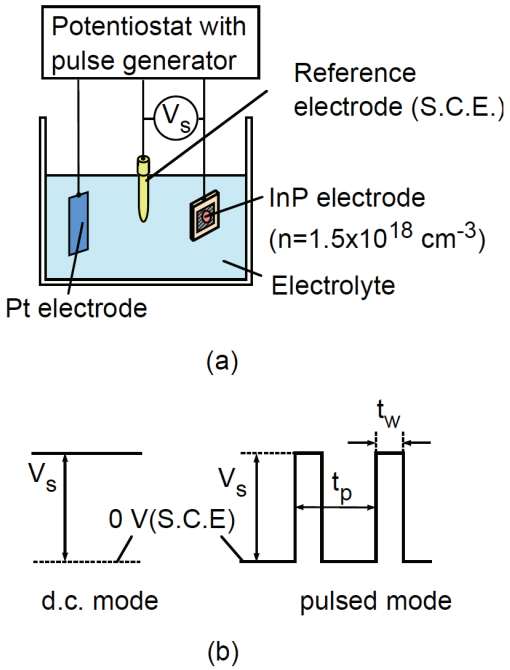

Fig. 2 (a) Setup of the electrochemical process for template formation and (b) the potential waveform used for electrochemical anodization.

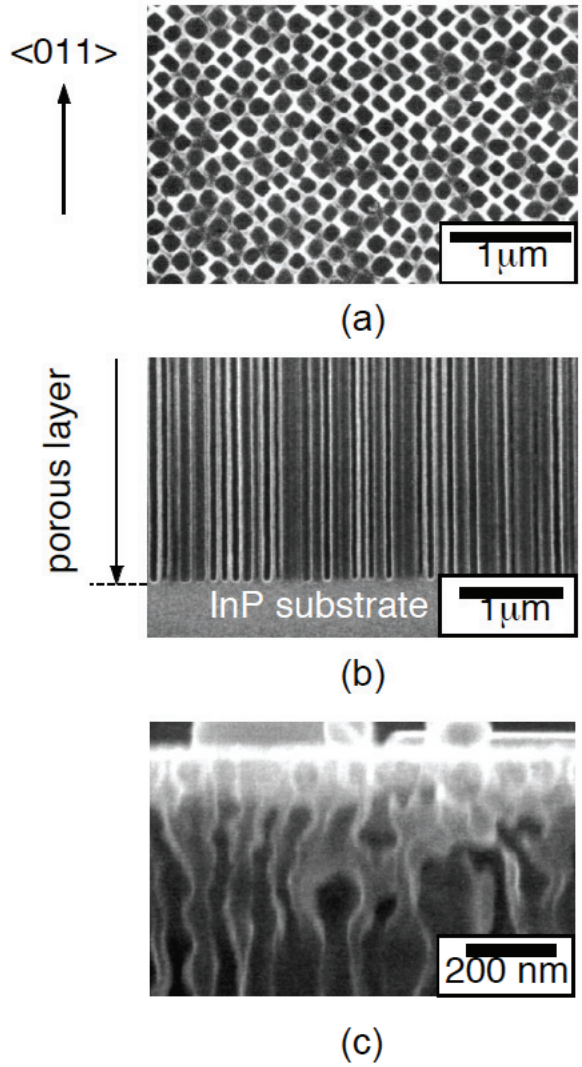

Fig. 3 Typical SEM images of porous InP structure: (a) plan-view, (b) cross-section (bottom) and (c) cross-section (top).

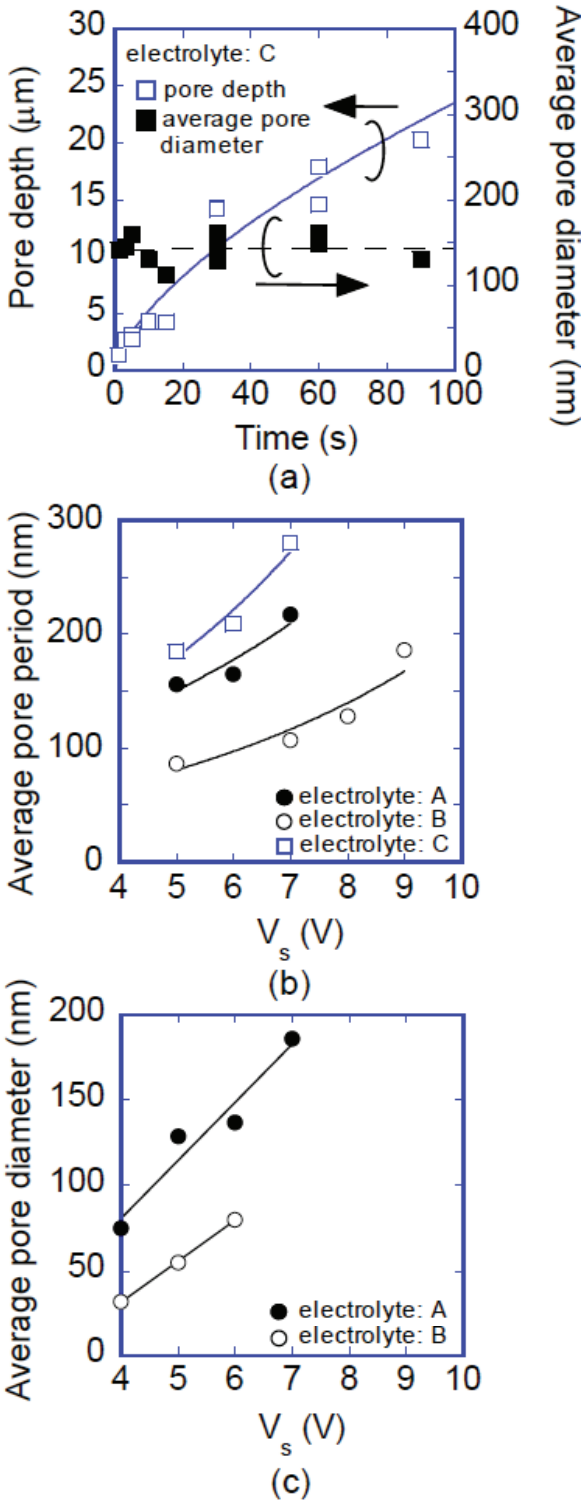

Fig. 4 (a) Pore depth and average pore diameter as functions of anodization time. (b) Average pore period and (c) average pore diameter as functions of applied bias.

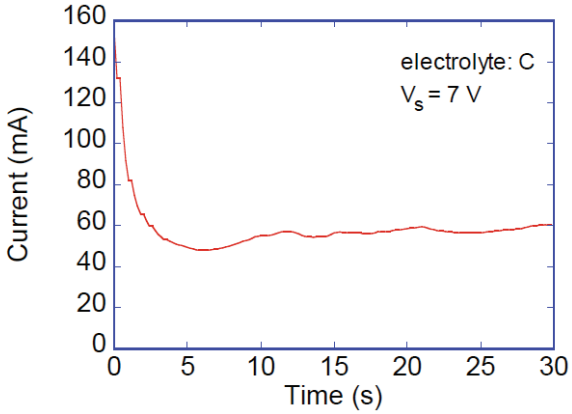

Fig. 5 Anodization time dependence of anodic current of porous formation.

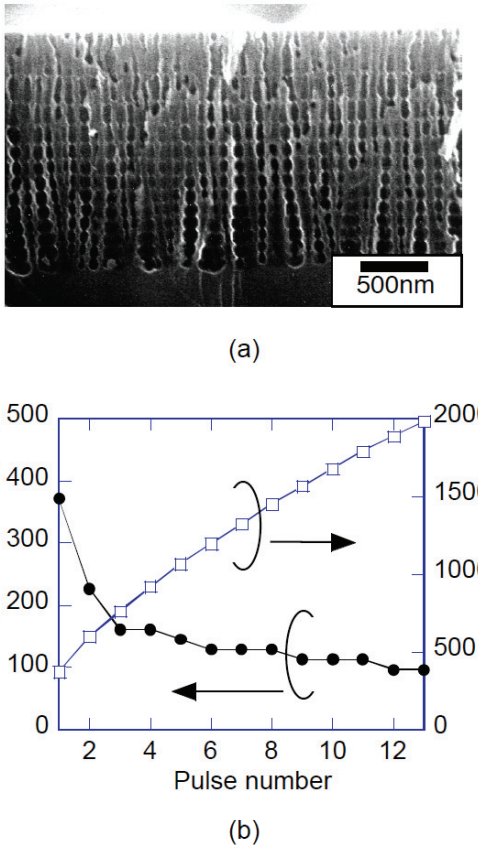

Fig. 6 (a) Cross section of InP pore template formed by the pulsed mode and (b) pore depth as functions of the number of applied pulses.

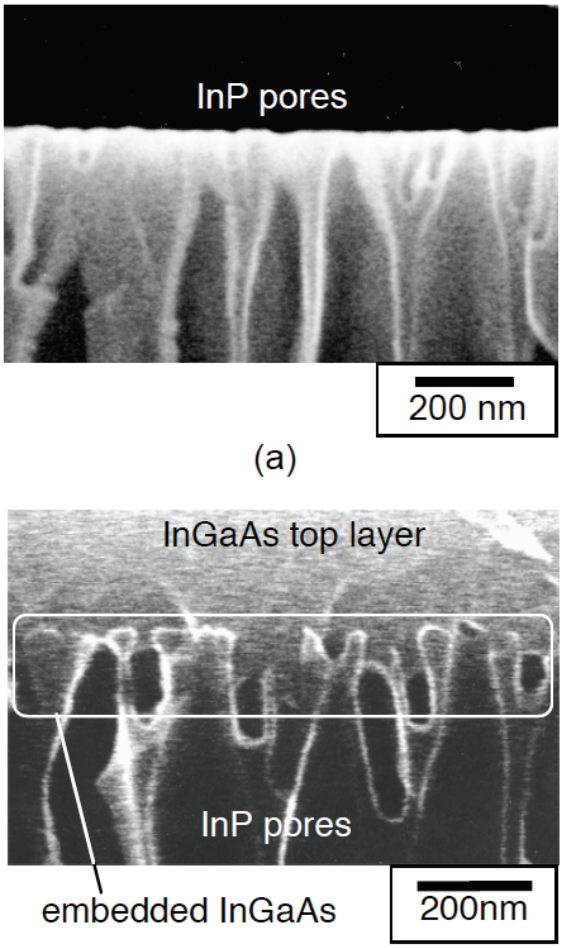

Fig. 7 Cross section of (a) InP pore template and (b) InGaAs/InP template after MBE growth.

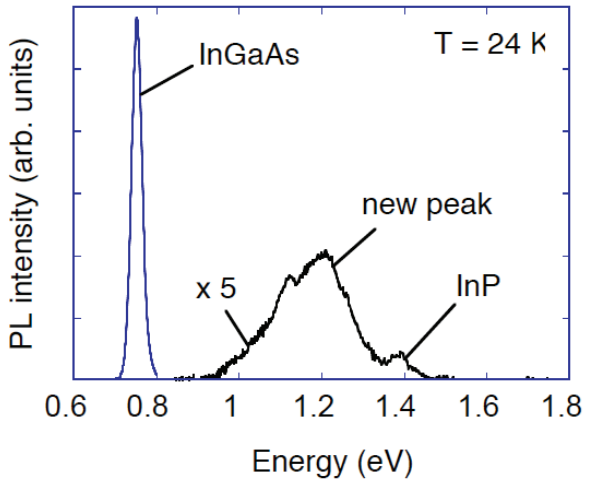

Fig. 8 PL spectra from InGaAs/InP template formed by MBE.